Chemical Science

ROYAL SOCIETY OF CHEMISTRY

EDGE ARTICLE

View Article Online
View Journal

Cite this: DOI: 10.1039/c9sc05050g

All publication charges for this article have been paid for by the Royal Society of Chemistry

Sodium caseinate as a particulate emulsifier for making indefinitely recycled pH-responsive emulsions†

Yongkang Xi,[a] Bo Liu,[a] Hang Jiang,[b] Shouwei Yin, *[abc] To Ngai *[b] and Xiaoquan Yang [ac]

Received 7th October 2019
Accepted 16th March 2020

DOI: 10.1039/c9sc05050g

rsc.li/chemical-science

pH-responsive emulsions are one of the simplest and most readily implementable stimuli-responsive systems. However, their practical uses have been greatly hindered by cyclability. Here, we report a robust pH-responsive emulsion prepared by utilizing pure sodium caseinate (NaCas) as the sole emulsifier. We demonstrate that the emulsification/demulsification of the obtained NaCas-stabilized emulsion can be triggered by simply changing the pH value over 100 cycles, which has never been observed in any protein-stabilized emulsion system. The NaCas-stabilized emulsion maintains its pH-responsive properties even in a saturated salt solution (NaCl ~ 6.1 M) or seawater. We illustrate how NaCas functions in pH-responsive emulsions and show that when conventional nanoparticles such as zein protein or bare SiO_2 particles were coated with a layer of NaCas, the resulting formulated emulsions could be switched on and off over 10 cycles. The unique properties of NaCas thus enable the engineering of conventional Pickering emulsions to pH-responsive Pickering emulsions. Finally, we have integrated catalytically active gold (Au) nanoclusters (NCs) into the NaCas protein and then utilized them to produce emulsions. Remarkably, these NaCas–Au NCs assembled at the oil–water interface exhibited excellent catalytic activity and cyclability, not only in aqueous solution, but also in complicated seawater environments.

Introduction

Emulsions are liquid-in-liquid droplets stabilized by emulsifiers, proteins, polymers or solid particles. Their size distributions range from several nanometers to hundreds of micrometers.[1–3] They have traditionally been employed as delivery systems[4] in the cosmetic,[5] food,[6] and pharmaceutical industries[7] and have emerging applications, such as templates for new material synthesis[8,9] and as nano- or microscale reactors for interface catalysis.[10,11] For emulsion interface catalysis (EIC), the efficient separation and recycling of catalysts are one of the major objectives of sustainable and green chemistry.[12,13] However, the catalysts in EIC have traditionally been separated and recycled *via* centrifugation and filtration, which are time- and energy-consuming. To address this issue, engineered "smart" emulsifiers, in particular inorganic or polymeric particles, have been developed recently to produce emulsions that are responsive to external stimuli such as pH,[12] temperature,[14] light,[15] and chemical agents.[16,17] Smart emulsifiers facilitate catalyst separation and recycling, making chemical processes more sustainable and environmentally friendly.

Among stimuli-responsive emulsion systems, particular interest has been devoted to the development of pH-responsive emulsions, as they are one of the simplest and most readily implementable stimuli-responsive systems.[12,18] Very often, however, pH-response cycles can only be performed several times due to the inherent increase in ionic strength caused by the repeated addition of acids and bases during the cycle. Moreover, the increased addition of free ions screens the charge of the emulsifiers, causing them to aggregate and eventually lose their function as the emulsifier.[18–21] Replacing the water phase repeatedly is often applied to decrease the ionic strength in cyclic systems, but it only partially addresses the issue. In addition, the used emulsifiers, such as silica, starch and ZnO nanoparticles (NPs), need surface functionalization, which involves more intensive procedures and the cyclability is often limited to less than 10 cycles.[20–22] Therefore, the development of efficient strategies for constructing green and sustainable pH-responsive emulsion catalytic systems is of ever increasing importance.

[a]Research and Development Centre of Food Proteins, School of Food Science and Engineering, Guangdong Province Key Laboratory for Green Processing of Natural Products Safety, South China University of Technology, Guangzhou, 510640, P. R. China. E-mail: feysw@scut.edu.cn

[b]Department of Chemistry, The Chinese University of Hong Kong, Shatin, N. T., Hong Kong. E-mail: tongai@cuhk.edu.hk

[c]Overseas Expertise Introduction Center for Discipline Innovation of Food Nutrition and Human Health (111 Center), Guangzhou 510640, PR China

† Electronic supplementary information (ESI) available: Experimental details and results. See DOI: 10.1039/c9sc05050g

Herein, we report a robust pH-responsive ethyl acetate-in-water emulsion prepared by using pure sodium caseinate (NaCas) as the particulate emulsifier. We found that stabilization and destabilization of the obtained NaCas-stabilized emulsion can be unprecedentedly triggered by simply tuning the pH value of the solution and that this cyclability maintained over 100 cycles. NaCas was also demonstrated to be a good emulsifier for stabilizing different oils, including toluene, benzene and dichloromethane and all emulsions could be switched on or off within one minute. We examined the specificity of the emulsion stabilized by NaCas by comparing the emulsions stabilized with other six common proteins including bovine serum albumin (BSA), whey protein isolate (WPI), gelatin, soybean protein isolate (SPI), zein, and sericin in order to reveal how NaCas functions at the interface in regulating the emulsion stability. Finally, as a proof of concept, we attempted to prepare an Au/NaCas catalyst (NaCas–Au) by *in situ* growing Au NCs onto NaCas, and we then tested the use of the as-prepared nanoparticles in formulation of emulsions for interfacial catalysis. We also evaluated their switchable cyclability in sensitive and complicated environments, such as the saturated salt solution or seawater.

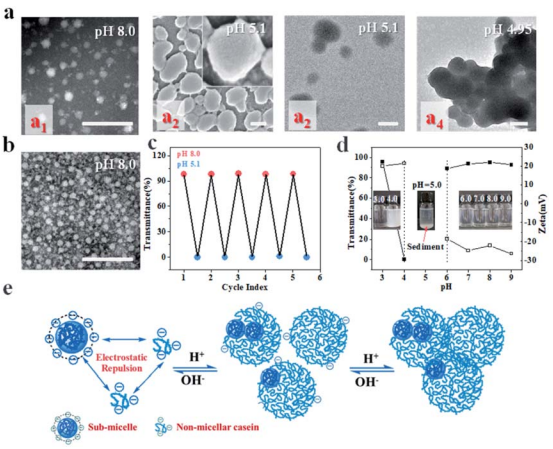

Fig. 1 pH-responsive performance of NaCas in deionized water. (a) pH-triggered morphological evolution of NaCas: TEM image at pH 8.0 (a_1), SEM image at 5.1 (a_2), TEM image at 5.1 (a_3), and TEM image at 4.95 (a_4). (b) TEM image of NaCas at pH 8.0 after 10 cycles of switching the pH value between 8.0 and 5.1. (c) Reversible transmittance change of the NaCas solution upon cycling between pH 8.0 and pH 5.1. (d) Zeta potential and transmittance % *T* of NaCas (0.05 wt%) as a function of pH. (e) A schematic representation of pH-switchable submicelle-aggregate conversion. Scale bar, 200 nm.

Results and discussion

Reversible pH-responsive association–disassociation of NaCas

Casein used in this work is a family of intrinsically disordered proteins (IDPs) including αs_1- and αs_2-caseins (collectively called α-casein), β-casein, and κ-casein. αs_1-casein is a triblock copolymer, and monomeric β-casein and κ-casein have both hydrophobic and hydrophilic extremities.[23–29] NaCas, which is derived from casein and has a highly disordered structure, is a robust amphipathic protein that typically associates into spherical micelles (sub-micelles) with diameters in the range of 20–40 nm under neutral and weakly basic conditions (for example, pH 8.0) (Fig. 1a_1). The sub-micelles can evolve to a 200–300 nm colloidal architecture decorated with small dots (Fig. 1a_2 inset) when the pH shifts to 5.1, and they form a cluster-like structure when the solution is further decreased (Fig. 1a_4) and finally precipitate during storage (Fig. 1d). It was very exciting to find that this association behaviour was fully reversible when the pH was adjusted back to 8.0 (Fig. 1c). Fig. 1b shows that NaCas actually can regain its original morphology even after 10 cycles. On the other hand, we noted that the intermediate colloidal architecture formed at pH 5.1 returned to the uniform sub-micelles with particle sizes of 20–40 nm after dilution (Fig. S1†), reflecting that the sub-micelles flocculated during acidification but did not coalescence or merge.

pH-responsive emulsions solely stabilized by NaCas

Inspired by the reversible association–disassociation behaviour of NaCas at different pH values as mentioned, we conjecture that pH-switchable emulsions can be constructed using NaCas as the particulate emulsifier. To test our hypothesis, a typical oil-in-water (o/w) emulsion with equal volume fractions of ethyl acetate/water was prepared by shearing the mixtures at a stirring rate of 15 000 rpm for 1 min. The as-prepared emulsion stabilized by 0.1 wt% of NaCas was stable at pH 8.5, and complete macroscopic phase separation occurred within 1 min upon adjusting the pH to 4.6–5.1 (ESI Movies 1–3†). This system, however, rapidly restored the emulsion (o/w) when a few drops of NaOH solution were added and the pH of the water phase was adjusted to 8.5. Remarkably, this emulsion could be reversibly switched on and off over 100 cycles (Fig. 2a). The type and droplet size of the regenerated emulsions were almost the same as those of the original emulsions (Fig. 2a), suggesting that the emulsifying performance of NaCas remained unchanged throughout all the cycles. Optical microscopy and scanning electron microscopy (SEM) images confirmed that after the first and tenth cycles, the agglomerates between the ethyl acetate and water layers observed after demulsification were flocs of NaCas (Fig. S2†). Next, we examined the effect of high salt concentration on this stimuli-responsive system, as salts usually promote the flocculation of emulsifiers and could passivate the cyclic system. As shown in Fig. 2b, quite surprisingly, the pH-responsive process functioned well in the presence of 6.1 M NaCl (saturated solution) for at least 5 runs (Fig. 2b). Therefore, our system could theoretically be recycled indefinitely since only water and salt were introduced throughout the cycle. Furthermore, the pH-responsive process functioned well when simulated seawater was used as the solvent for at least 5 cycles (Fig. 2c), indicating that we established an extraordinary and robust pH-responsive emulsion system using NaCas as the particulate emulsifier.

Universality and potential applications of this strategy

In addition to the ethyl acetate/water system, we found that NaCas was also a good emulsifier for stabilizing other oils,

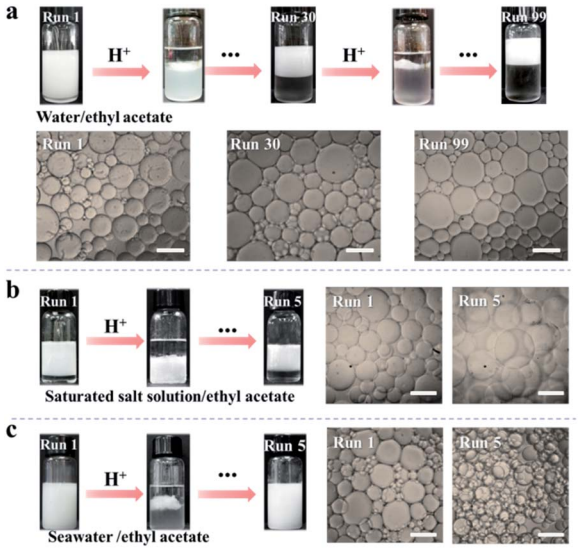

Fig. 2 pH-responsive emulsions stabilized by NaCas. (a) Appearance and optical micrographs of successive pH-responsive NaCas-stabilized emulsion (0.1 wt%) conversion cycles using ethyl acetate as the oil phase (1st, 30th and 99th cycle). (b) Appearance and optical micrographs of emulsions stabilized by NaCas using a saturated salt solution as the solvent. (c) Appearance and optical micrographs of emulsions stabilized by NaCas using seawater as the solvent. Scale bar, 30 μm.

including toluene, benzene and dichloromethane (Fig. S3†). In these systems, all emulsions could be switched on or off through the regulation of the pH value. Demulsification was accomplished within one minute under stirring and the type and droplet size of the regenerated emulsions remained almost the same during and after 10 cycles (Fig. S3†).

Specificity of pH-responsive emulsions stabilized by NaCas

Why could NaCas-stabilized emulsions be cycled nearly infinitely? To answer this question, we constructed a series of emulsions using 6 representative proteins, including three animal proteins: BSA, WPI and, gelatin, two plant proteins: SPI and zein, and an insect protein, sericin, and investigated the pH-triggered switchability of the as-prepared emulsions. Typically, ethyl acetate as the oil phase was mixed with protein solutions (pH 8.5, 0.1 wt%) at an equal volume fraction, and then the resulting mixtures were sheared at a stirring rate of 15 000 rpm for 1 min. The pH-switchable performance of the as-prepared emulsions was then assessed. Regrettably, the emulsions stabilized by BSA, WPI, SPI and sericin did not break when the pH was adjusted to 4.6–5.1, while no stable emulsions were developed at pH 8.5 for gelatin with the abovementioned procedure (Fig. S4a†). For emulsions stabilized by zein colloidal particles (ZCPs), the cycle could be switched on and off for only 2 times, and oil leakage occurred quickly after further emulsification (Fig. S4b†). Obvious agglomerates were observed in microscopic images of the emulsions after the 2nd cycle (Fig. S4c†). We thereby surmise that the unique pH-responsive behaviour of NaCas-stabilized emulsions as well as the indefinitely reversible association–disassociation behaviour should be mainly attributed to the specific protein structure of NaCas.

Working principle for pH-responsive emulsions stabilized by NaCas

To understand the specifics of the emulsion stabilized by NaCas, we applied cryo-SEM to examine the NaCas behavior at the oil–water interface. Fig. 3 shows representative cryo-SEM images of emulsions with ethyl acetate as the oil phase at both pH 5.5 and 8.0. During sample fracture, the frozen ethyl acetate constituting the droplet was removed, forming a cavity and allowing direct visualization of the configuration of NaCas residing at the interface. For the emulsions at pH 8.0, spherical shells with regularly spaced bumps were clearly visualized, reflecting that the interfacial layer was characterized by the complex architecture of sub-micelles and flexible caseins (Fig. 3b_1 and 3b_2). In contrast, the droplets tended to deform and coalesce at pH 5.5, and the cryo-SEM image directly reflected that the emulsions were close to the threshold of phase separation (Fig. 3b_3). NaCas at this pH adopted an unordered agglomerate configuration (Fig. 3b_4). During sublimation, the interfacial architecture collapsed, possibly due to the limited coverage of emulsifiers (Fig. 3b_3). Cryo-SEM images of emulsions with dodecane as the oil phase at different pH values revealed that NaCas formed a dense interfacial film to stabilize the emulsions under alkaline conditions (Fig. S5a_1 and a_2†). Instead, they formed a torn and porous film as well as aggregates at the interface after adjusting the pH to 4.8 (Fig. S5b_1 and

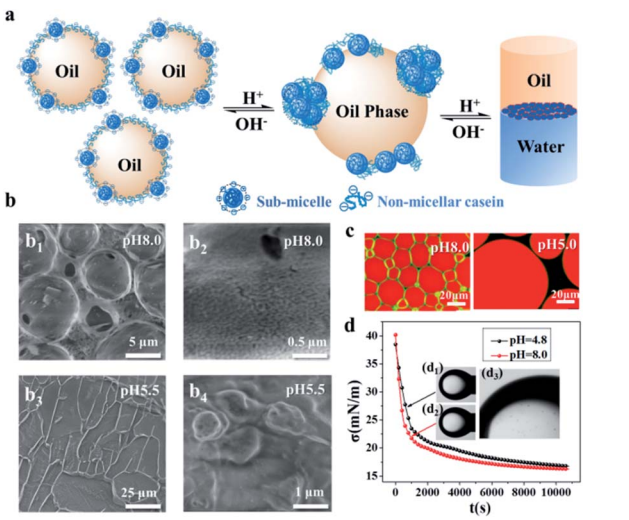

Fig. 3 Mechanism of pH-responsive emulsions stabilized by NaCas. (a) Schematic illustration of the pH-responsive emulsion system stabilized by NaCas. (b) Cryo-SEM images of emulsions stabilized by NaCas: (b_1 and b_2) cryo-SEM image of emulsion droplets at pH 8.0; (b_3 and b_4) cryo-SEM image of emulsion droplets at pH 5.5. (c) CLSM image of NaCas-stabilized emulsions using dodecane as the oil phase at pH 8.0 and 5.0. (d) The change in interfacial tension with time using dodecane as the oil phase at different pH (d_1 and d_2). Droplet images of NaCas solutions at different pH values. A large number of flocs were present in the droplets at pH 4.8 (d_3).

b_2†). This result was also supported by CLSM images showing that as the pH was shifted to 5.0 (Fig. 3b) and 4.0 (Fig. S6†), the thickness of the interfacial protein layers decreased, and aggregates of NaCas appeared in the aqueous phase. In addition, as shown in Fig. 3d, NaCas had similar interfacial tension (16.80 and 16.30 mN m^{-1}) and adsorption rates (0.636 and 0.948 mN m^{-1} $S^{-0.5}$) at pH 4.8 and 8.0, indicating that demulsification was not due to the decrease in the interfacial activity of the emulsifier.

A schematic illustration of the working principle for the pH-responsive emulsion system is proposed in Fig. 3a. NaCas is classified as an IDP with an open conformation.[24] Individual casein molecules are highly amphiphilic, triblock copolymers with a high proportion of accessible non-polar residues. Due to the amphiphilicity, they could be adsorbed at the interface and produce stable o/w emulsions. Protonation and deprotonation make the hydrophilicity/hydrophobicity of NaCas switchable, thereby driving the reversible pH-responsive emulsification/demulsification of the NaCas-stabilized emulsions. It is worth mentioning that most proteins have a considerably ordered secondary structure with a compact tertiary structure and usually feature hydrophobic groups folded in their interior. Thus, rapidly forming and disrupting emulsions stabilized by these compact proteins on command remain a challenge. In contrast, caseins have an open conformation and no tertiary structure. In addition, caseins have a number of Ser(P) residues in specific phosphorylation-site motifs, such as [-(Ser(P)-)3 (Glu-)2].[30–32] Inductively coupled plasma (ICP) investigations confirmed that the content of phosphorus in NaCas was 3.45 wt%. When the pH was shifted to neutral or alkaline values, deprotonation of the phosphoserine clusters inside the agglomerates made them highly negatively charged. Such an electrostatic repulsion should lead to the agglomerates to disperse into a sub-micelle state. This is why the NaCas-stabilized emulsion can be formed and broken within 1 min. Furthermore, the phosphoserine clusters can dynamically bind to the positive ions to form a positively charged layer around the localized micelles, serving as a vehicle for capturing ions,[33–35] providing theoretical support for strong salt tolerance, and thus contributing to the indefinitely reversible pH-responsive cyclability (Fig. S7†) that cannot be found in other common proteins.

NaCas-modified organic or inorganic particles for shaping robust pH-responsive emulsions

Understanding how NaCas functions in pH-responsive emulsions provides us a further tool to engineer emulsions even if they are stabilized by conventional solid particles. To demonstrate this, NaCas was physically adsorbed onto hydrophobic zein particles (zein–NaCas) or hydrophilic bare SiO_2 particles (SiO_2–NaCas) and then used to stabilize o/w emulsions. Fig. 4 and S8† show that the emulsions stabilized by NaCas-modified zein–NaCas or SiO_2–NaCas could be switched on and off over 10 cycles. SEM images show that the interfacial layer of the emulsions was covered by the well-defined silica (SiO_2–NaCas see Fig. $4a_2$) or zein colloidal particles (zein–NaCas see Fig. $4b_2$), which was further confirmed by CLSM images derived from

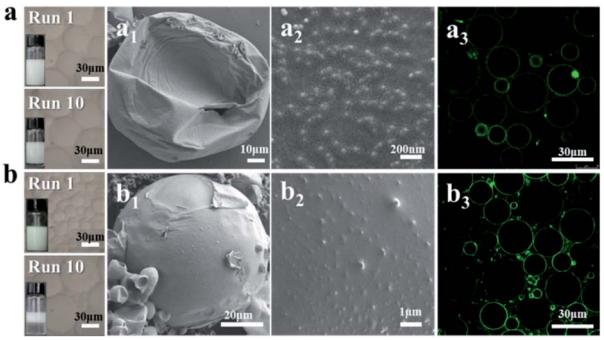

Fig. 4 pH-responsive emulsions stabilized by SiO_2–NaCas and zein–NaCas. (a) Appearance and optical micrographs of successive pH-responsive SiO_2–NaCas stabilized emulsion (0.004 wt% NaCas and 0.02 wt% SiO_2) conversion cycles using ethyl acetate as the oil phase (1st and 10th cycle). (a_1–a_3) SEM (a_1 and a_2) and CLSM (a_3) image of the emulsion stabilized by SiO_2–NaCas. (b) Appearance and optical micrographs of successive pH-responsive zein–NaCas -stabilized emulsion (0.1 wt% zein–NaCas) conversion cycles using ethyl acetate as the oil phase (1st and 10th cycle). (b_1–b_3) SEM (b_1 and b_2) and CLSM (b_3) image of the emulsion stabilized by zein–NaCas.

FITC-labelled silica (Fig. $4a_3$) and FITC-labelled zein (Fig. $4b_3$). Our finding thus enables the engineering of conventional Pickering emulsions stabilized by bare SiO_2 or zein nanoparticles to pH-responsive Pickering emulsions, which will open a new avenue to explore their applications in heterogeneous catalysis.

Recyclable interfacial catalysis

The above studies demonstrate that we have established a NaCas-stabilized emulsion system which can tolerate a variety of oils, having infinitely switchable cyclability, and undergoing rapid and facile demulsification, even in sensitive and complicated environments, such as a saturated salt solution or seawater. One may wonder if these properties are favourable for designing efficient and recyclable catalytic systems. As a proof of concept, we attempted to prepare an Au/NaCas catalyst (NaCas–Au) by *in situ* growing Au NCs onto NaCas, and we then tested the use of the as-prepared nanoparticles in formulation of emulsions for interfacial catalysis. As shown in Fig. S10,† NaCas–Au revealed a spheroidal structure with a particle size of 20–40 nm under alkaline conditions. In addition, scanning transmission electron microscopy (STEM) energy-dispersive X-ray spectroscopy (EDX) mappings of NaCas–Au confirmed that Au NCs were successfully loaded on NaCas because several elemental peaks are basically coincident (Fig. 5a and a_1–a_4). According to ICP-AES, the loading of Au NCs in NaCas–Au was 2.35 wt%. High-resolution transmission electron microscopy (HR-TEM) analysis further confirmed that Au NCs (Fig. 5b and b_1) were anchored evenly over the NaCas hosts and had essentially a narrow and monodisperse profile with a mean diameter of 1.4 nm (Fig. 5c and c_1).

This finding was further supported by the absence of a peak at 520 nm in the UV-vis spectra (Fig. S11†) of NaCas–Au NCs. In fact, when the Au particle size was less than 5 nm, there was no

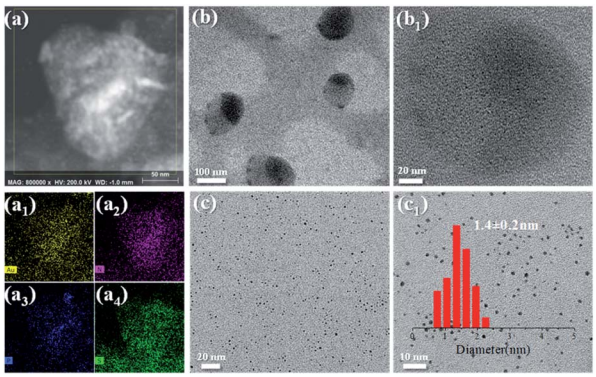

Fig. 5 STEM EDX mappings of NaCas–Au NCs. Au, N, P, and S signals are given in a_1, a_2, a_3, and a_4, respectively. TEM images of NaCas–Au NCs at pH 5.1 (b and b_1) and 8.0 (c and c_1).

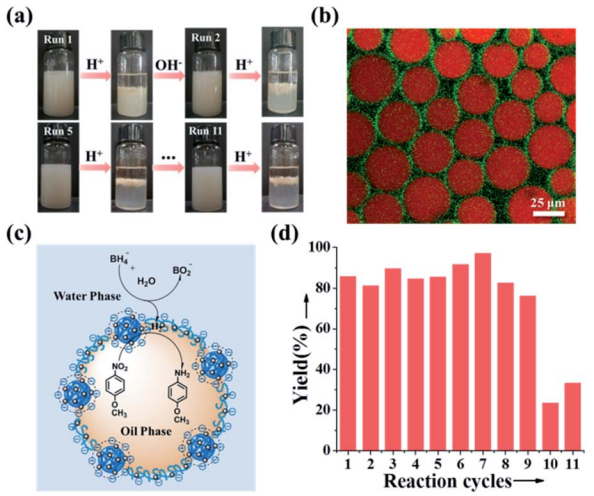

Fig. 6 Recyclable interfacial catalysis *via* NaCas–Au NCs. (a) Photographs of successive pH-responsive NaCas–Au NC-stabilized emulsion (0.1 wt%) conversion cycles using ethyl acetate as the oil phase (1st, 2nd, 5th and 9th cycle). (b) CLSM images of emulsions stabilized by NaCas–Au NCs. (c) Catalytic mechanism of the emulsion stabilized by NaCas–Au NCs. (d) Recycling results for the catalytic hydrogenation of *p*-nitroaniline by interfacial NaCas–Au NCs in the ethyl acetate/water system. The reaction time was 15 min.

absorption peak corresponding to the surface plasmon resonance at 300–650 nm.[36] Moreover, these results were in good agreement with the XRD profiles, where the NaCas–Au NCs presented a smooth diffraction peak at $2\theta = 35–45°$ (Fig. S12;† a crystalline species usually presents a sharp peak here).[37] X-ray photoelectron spectroscopy (XPS) was used to characterize the Au state. The Au^0 $4f_{7/2}$ and $4f_{5/2}$ peaks are centred at 84.3 eV and 88.1 eV, respectively, while the peaks at approximately 85.5 eV and 89.1 eV correspond to Au^+ species. XPS data suggested that all of the Au^{3+} precursor was fully reduced to form Au NCs (Fig. S13†).[38,39]

It is generally accepted that NaCas is rich in functional groups such as amino and carboxyl groups that could bind Au^{3+} ions through ionic and covalent interactions, confining the nucleation and growth of Au NCs with a relatively small size. The Fourier transform infrared (FT-IR) results verified the interactions between NaCas and the Au NCs (Fig. S14†). Fig. S15† shows a possible formation mechanism of the NaCas–Au NCs.

To verify whether NaCas still had excellent emulsification and pH-responsive conversion properties after loading Au NCs, we adjusted the pH in the oil–water system back and forth between the isoelectric point (pH = 4.8; the isoelectric point before and after the loading did not change significantly; Fig. S16†) and alkaline pH. We noted that pH-responsive conversion can be continuously cycled more than 11 times (we did perform only 11 cycles). Compared with that of bare NaCas, the pH-responsive conversion ability of NaCas–Au NCs did not decrease (Fig. 6a).

NaCas–Au NCs were used as the emulsifier, and the hydrogenation of *p*-nitroanisole in an ethyl acetate/aqueous biphasic system was used as a model reaction to evaluate the catalytic efficiency, separability and recyclability of the catalyst. Before the reaction, the biphasic pH value was adjusted to 8.5, and then NaCas–Au NC-stabilized emulsions were formed after homogenization. Under this condition, *p*-nitroanisole was encapsulated in the dispersed droplets stabilized by the NaCas–Au NCs. These dispersed oil droplets were considered as many individual pH-responsive microreactors, where Au NCs at the oil–water interface catalysed the transformation of substrates into products in the oil phase. Separation of the products from the reaction system was easy to achieve by adjusting the pH value to 4.8 using a few drops of HCl solution to break the emulsion. In this way, NaCas–Au NCs were observed to transfer to the boundary within one minute, and the upper oil phase could be separated through simple decantation.

Subsequently, we further evaluated the catalytic efficiency of this emulsion system through a comparison between Au NPs and NaCas–Au NCs, which are schematically illustrated in Fig. S19 and S21† (the real-time data obtained by gas chromatography (GC) are shown in Fig. S17–S21†). As shown in Fig. S20,† the substrate peak (*p*-nitroanisole) at 5.5 min almost disappeared after 5 min of catalytic reaction, and a strong and sharp peak (*p*-anisidine) at 2.6 min appeared concomitantly. To further explore the purity of our catalytic products, we used gas chromatography and mass spectrometry (GC-MS) to identify the products (Fig. S20†). Most pleasingly, we noted that the product of the catalytic reaction was *p*-anisidine and that its content was 100%. Our findings led us to conclude that the NaCas–Au NCs had specificity for the catalytic hydrogenation of *p*-nitroanisole to produce *p*-anisidine. Regarding the Au NP catalytic system, the conversion rate was still less than 50% when the reaction was carried out for 30 min (Fig. S21†), which was much slower than that of the o/w emulsion system stabilized by NaCas–Au NCs. On the one hand, the superiority in reaction efficiency mainly originated from the enhanced contact region facilitated by emulsion formation, along with the consequently increased mass transfer frequency between the two phases (Fig. 6b). Au NCs displayed a green signal at the oil–water interface, and the oil presented a red signal. We found that a green aperture

surrounds the red oil droplets, suggesting that NaCas–Au NCs attached to the oil–water interface when forming emulsions. The mechanism of the interfacial catalytic reaction is shown in Fig. 6c. On the other hand, according to previous research, the catalytic activity of Au particles decreases exponentially with increasing Au particle size,[40,41] and the size of the Au NPs without NaCas (Fig. S22a, a_1 and a_2,† average particle diameter 5.2 nm) is significantly larger than that of the Au NCs in NaCas–Au NCs (Fig. 5, average particle diameter 1.4 nm), which could result in decreased catalytic efficiency.

To recycle the catalyst, fresh substrates were added, and the pH was re-adjusted to 8.5. To our delight, this pH-responsive NaCas–Au NC-stabilized emulsion system was highly recyclable, which was highlighted by the high yields obtained over at least 9 reaction cycles (Fig. 6d and S23†), and all yields were more than 80%. Unfortunately, a slight reduction in yield happened after 9 cycles, mainly because sodium borohydride was used as a hydrogen source in this experiment, which inevitably led to an increase in the size of the Au NCs on NaCas (the size of the Au NCs increased from 1.4 ± 0.6 nm to 3.8 ± 0.6 nm after 9 cycles, becoming Au NPs; Fig. S22b, b_1 and b_2†). More importantly, these NaCas–Au NCs at the oil–water interface also exhibited excellent catalytic activity in sensitive and complicated environments, such as a saturated salt solution or seawater. The yields were more than 80% (Table S1†). Moreover, the ability of NaCas to cap metals was generalizable to other metals such as Pd and Rh. The resultant NaCas–Pd and NaCas–Rh catalysts also showed activity and could be recycled by the pH-triggered strategy (Table S2†).

Conclusion

We have successfully developed a robust pH-responsive emulsion prepared by using pure NaCas as the sole emulsifier. Unlike conventional proteins, NaCas is an IDP with unique open conformation. Another attractive feature is the intrinsic presence of the specific phosphorylation-site motifs, such as [-(Ser(P)-)3 (Glu-)2] of NaCas. The hydrolysis leads to casein phosphopeptide (CPP) which could be used as a vehicle for ion capture, providing theoretical support for strong salt tolerance formation and resulting in nearly infinite cyclability that has never been observed in any protein-stabilized emulsions. We also demonstrate that NaCas can be universally applied to stabilize many other kinds of oils, including toluene, benzene and dichloromethane, and the resultant emulsions could be switched on or off through the regulation of the pH value within one minute under stirring. The unique properties of NaCas discovered in this study provide a new chapter for the engineering of novel pH-responsive emulsions whether they are stabilized by conventional solid or soft nanoparticles. Thus, this reversible pH-switchable emulsion system could be extensively used in heterogeneous catalysis, crude oil recovery and delivery.

As a proof of concept, we demonstrate a process combining a green and sustainable catalytic reaction and product separation in a single reaction vessel through emulsification/demulsification conversion triggered by pH. Regarding catalyst separation and recycling, this method saves time and energy. The high stability of the system is highlighted by its robustness over 100 cycles and high salt tolerance. With this successive catalyst separation and recycling system, the overall efficiency of a chemical process may be significantly improved, and the work-up method may be simplified. This pH-triggered conversion platform could be readily extended to other interfacial catalytic systems, such as carrier enzyme catalysis, supported bimetallic catalysis and even synergistic catalysis of supported metals and enzymes. In addition, the key advantage of the carrier in this platform is that it is a natural protein, which provides the possibility of the catalytic production of products such as food and medicines, in accordance with the concept of green and sustainable chemistry. Therefore, this strategy may open interesting avenues for establishing green and sustainable platforms with various recyclable catalysts and separation products.

Conflicts of interest

There are no conflicts to declare.

Acknowledgements

This work was financially supported by the Hong Kong Special Administration Region (HKSAR) General Research Fund (CUHK14306617 and 2130535), and the project granted by the National Natural Science Foundation of China (31471628).

Notes and references

1 B. P. Binks, *Modern aspects of emulsion science*, Royal Society of Chemistry, Cambridge, 1998.
2 P. Guillamat, Ž. Kos, J. Hardoüin, J. Ignés-Mullol, M. Ravnik and F. Sagués, *Sci. Adv.*, 2018, **4**, eaao1470.
3 S. M. Hashemnejad, A. Z. M. Badruddoza, B. Zarket, C. R. Castaneda and P. S. Doyle, *Nat. Commun.*, 2019, **10**, 2749–2758.
4 T. F. Tadros, *Applied surfactants: principles and applications*, Wiley-VCH, Weinheim, 2006.
5 O. Sonneville-Aubrun, J. T. Simonnet and F. L'alloret, *Adv. Colloid Interface Sci.*, 2004, **108**, 145–149.
6 D. J. McClements, *Soft Matter*, 2011, **7**, 2297–2316.
7 A. Spernath and A. Aserin, *Adv. Colloid Interface Sci.*, 2006, **128**, 47–64.
8 K. Min, H. Gao and K. Matyjaszewski, *J. Am. Chem. Soc.*, 2006, **128**, 10521–10526.
9 B. Y. Guan, L. Yu and X. W. Lou, *J. Am. Chem. Soc.*, 2016, **138**, 11306–11311.
10 W. Zhang and Q. Zhong, *J. Agric. Food Chem.*, 2009, **57**, 9181–9189.
11 H. Yang, L. Fu, L. Wei, J. Liang and B. P. Binks, *J. Am. Chem. Soc.*, 2015, **137**, 1362–1371.
12 H. Yang, T. Zhou and W. Zhang, *Angew. Chem., Int. Ed.*, 2013, **52**, 7455–7459.
13 Z. Sun, U. Glebe, H. Charan, A. Böker and C. Wu, *Angew. Chem., Int. Ed.*, 2018, **52**, 13810–13814.
14 L. Qi, Z. Luo and X. Lu, *Green Chem.*, 2019, **21**, 2412–2427.

15 L. D. Zarzar, V. Sresht, E. M. Sletten, J. A. Kalow, D. Blankschtein and T. M. Swager, *Nature*, 2015, **518**, 520–524.
16 Y. Zhang, S. Guo, X. Ren, X. Liu and Y. Fang, *Langmuir*, 2017, **33**, 12973–12981.
17 Y. Liu, P. G. Jessop, M. Cunningham, C. A. Eckert and C. L. Liotta, *Science*, 2006, **313**, 958–960.
18 J. Tang, P. J. Quinlan and K. C. Tam, *Soft Matter*, 2015, **11**, 3512–3529.
19 H. Liu, C. Wang, S. Zou, Z. Wei and Z. Tong, *Langmuir*, 2012, **28**, 11017–11024.
20 L. Qi, Z. Luo and X. Lu, *Green Chem.*, 2018, **20**, 1538–1550.
21 Z. Y. Zhang, Y. D. Xu, Y. Y. Ma, L. L. Qiu, Y. Wang, J. L. Kong and H. M. Xiong, *Angew. Chem., Int. Ed.*, 2013, **52**, 4127–4131.
22 S. Fujii, Y. Cai, J. V. Weaver and S. P. Armes, *J. Am. Chem. Soc.*, 2005, **127**, 7304–7305.
23 D. J. McMahon and W. R. McManus, *J. Dairy Sci.*, 1998, **81**, 2985–2993.
24 E. Dickinson, *Int. Dairy J.*, 1999, **9**, 305–312.
25 D. L. Melnikova, V. D. Skirda and I. V. Nesmelova, *J. Phys. Chem. B*, 2017, **121**, 2980–2988.
26 J. Huang, L. Wang, R. Lin, A. Y. Wang, L. Yang, M. Kuang, W. Qian and H. Mao, *ACS Appl. Mater. Interfaces*, 2013, **5**, 4632–4639.
27 D. L. Melnikova, V. D. Skirda and I. V. Nesmelova, *J. Phys. Chem. B*, 2019, **123**, 2305–2315.
28 E. Dickinson, *Colloids Surf., A*, 2006, **288**, 3–11.
29 J. Surh, E. A. Decker and D. J. McClements, *Food Hydrocolloids*, 2006, **20**, 607–618.
30 C. G. De Kruif, T. Huppertz, V. S. Urban and A. V. Petukhov, *Adv. Colloid Interface Sci.*, 2012, **171**, 36–52.
31 K. J. Cross, N. L. Huq and E. C. Reynolds, *Biochemistry*, 2016, **55**, 4316–4325.
32 T. Wang, X. Chen, Q. Zhong, Z. Chen, R. Wang and A. R. Patel, *Adv. Funct. Mater.*, 2019, 1901830.
33 S. Perego, E. Del Favero, P. De Luca, F. Dal Piaz, A. Fiorilli and A. Ferraretto, *Food Funct.*, 2015, **6**, 1796–1807.
34 M. Ali Naqvi, K. Anaraki Irani, M. Katanishooshtari and D. Rousseau, *Curr. Protein Pept. Sci.*, 2016, **17**, 368–379.
35 V. A. Mittal, A. Ellis, A. Ye, P. J. Edwards and H. Singh, *Food Chem.*, 2018, **239**, 17–22.
36 Y. Liu, L. Liu, M. Yuan and R. Guo, *Colloids Surf., A*, 2013, **417**, 18–25.
37 T. G. Schaaff and R. L. Whetten, *J. Phys. Chem. B*, 1999, **103**, 9394–9396.
38 Y. Liu, Q. Yao, X. Wu, T. Chen, Y. Ma, C. N. Ong and J. Xie, *Nanoscale*, 2016, **8**, 10145–10151.
39 H. Kawasaki, K. Hamaguchi, I. Osaka and R. Arakawa, *Adv. Funct. Mater.*, 2011, **21**, 3508–3515.
40 B. Hvolbæk, T. V. Janssens, B. S. Clausen, H. Falsig, C. H. Christensen and J. K. Nørskov, *Nano Today*, 2007, **2**, 14–18.
41 M. Turner, V. B. Golovko, O. P. Vaughan, P. Abdulkin, A. Berenguer-Murcia, M. S. Tikhov, B. F. Johnson and R. M. Lambert, *Nature*, 2008, **454**, 981–983.